UV/Ozone-Oxidized Large-Scale Graphene Platform with Large Chemical Enhancement in Surface-Enhanced Raman Scattering

Sung Huh,[†] Jaesung Park,[‡] Young Soo Kim,[§] Kwang S. Kim,[‡] Byung Hee Hong,[§,⊥] and Jwa-Min Nam[†,*]

[†]Department of Chemistry, Seoul National University, Seoul 151-742, Korea, [‡]Department of Chemistry, Pohang University of Science and Technology, Pohang 790-784, Korea, and [§]SKKU Advanced Institute of Nanotechnology (SAINT), [⊥]Department of Chemistry, Sungkyunkwan University, Suwon 440-746, Korea

ABSTRACT

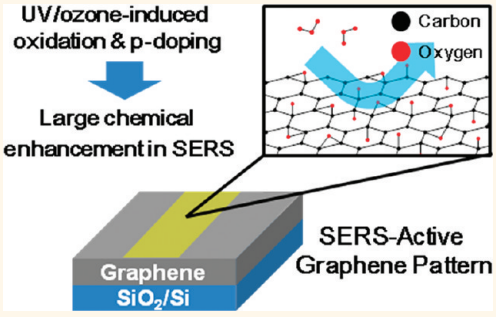

We fabricated a highly oxidized large-scale graphene platform using chemical vapor deposition (CVD) and UV/ozone-based oxidation methods. This platform offers a large-scale surface-enhanced Raman scattering (SERS) substrate with large chemical enhancement in SERS and reproducible SERS signals over a centimeter-scale graphene surface. After UV-induced ozone generation, ozone molecules were reacted with graphene to produce oxygen-containing groups on graphene and induced the p-type doping of the graphene. These modifications introduced the structural disorder and defects on the graphene surface and resulted in a large chemical mechanism-based signal enhancement from Raman dye molecules [rhodamine B (RhB), rhodamine 6G (R6G), and crystal violet (CV) in this case] on graphene. Importantly, the enhancement factors were increased from $\sim 10^3$ before ozone treatment to $\sim 10^4$, which is the largest chemical enhancement factor ever on graphene, after 5 min ozone treatment due to both high oxidation and p-doping effects on graphene surface. Over a centimeter-scale area of this UV/ozone-oxidized graphene substrate, strong SERS signals were repeatedly and reproducibly detected. In a UV/ozone-based micropattern, UV/ozone-treated areas were highly Raman-active while nontreated areas displayed very weak Raman signals.

KEYWORDS: graphene · oxidized graphene · ozone · surface-enhanced Raman scattering · chemical enhancement

Graphene has been intensively studied because of its unique and useful electrical, mechanical, and chemical properties.[1−4] One of its promising applications is the use of graphene as a substrate for the surface-enhanced Raman scattering (SERS),[5−8] and SERS has been used from single-molecule detection to multiplexed target detection applications.[9,10] In SERS, there are two widely accepted enhancement mechanisms—electromagnetic and chemical mechanisms (EM and CM), and it is difficult to separate these two mechanisms from each other. The EM is based on surface plasmon resonance (SPR) of metallic nanostructures and has been much more rigorously studied than the CM[11−14] because the contribution from the CM is typically much less than the EM, and separating the chemical contribution from the EM is difficult. Key to the separation of these two mechanisms could be the use of completely flat metallic substrate.[15] Graphene has many advantages as a substrate in studying the CM, and the advantages include an atomic flat surface that causes a small-distance charge transfer between the graphene surface and adsorbed molecules more reliably and efficiently, surface plasmon range in terahertz that enables separation the CM from the EM, and low manufacturing cost compared to other noble-metal-based SERS substrates.[16,17] Recently, there have been major breakthroughs in synthesizing large-scale graphene films using the chemical vapor deposition (CVD) method.[18,19] This CVD-grown large-scale graphene film can be an excellent SERS substrate because (1) it provides a large, atomic flat substrate for SERS studies; (2) conventional patterning techniques such as E-beam lithography and photolithography require a surface area of several tens of micrometer-scale for the site-selective SERS studies on patterned graphene substrates; and (3) the graphene can be transferred to an arbitrary substrate, such as a flexible polymer matrix.[20]

* Address correspondence to jmnam@snu.ac.kr.

Received for review August 29, 2011 and accepted November 9, 2011.

Published online November 09, 2011
10.1021/nn204156n

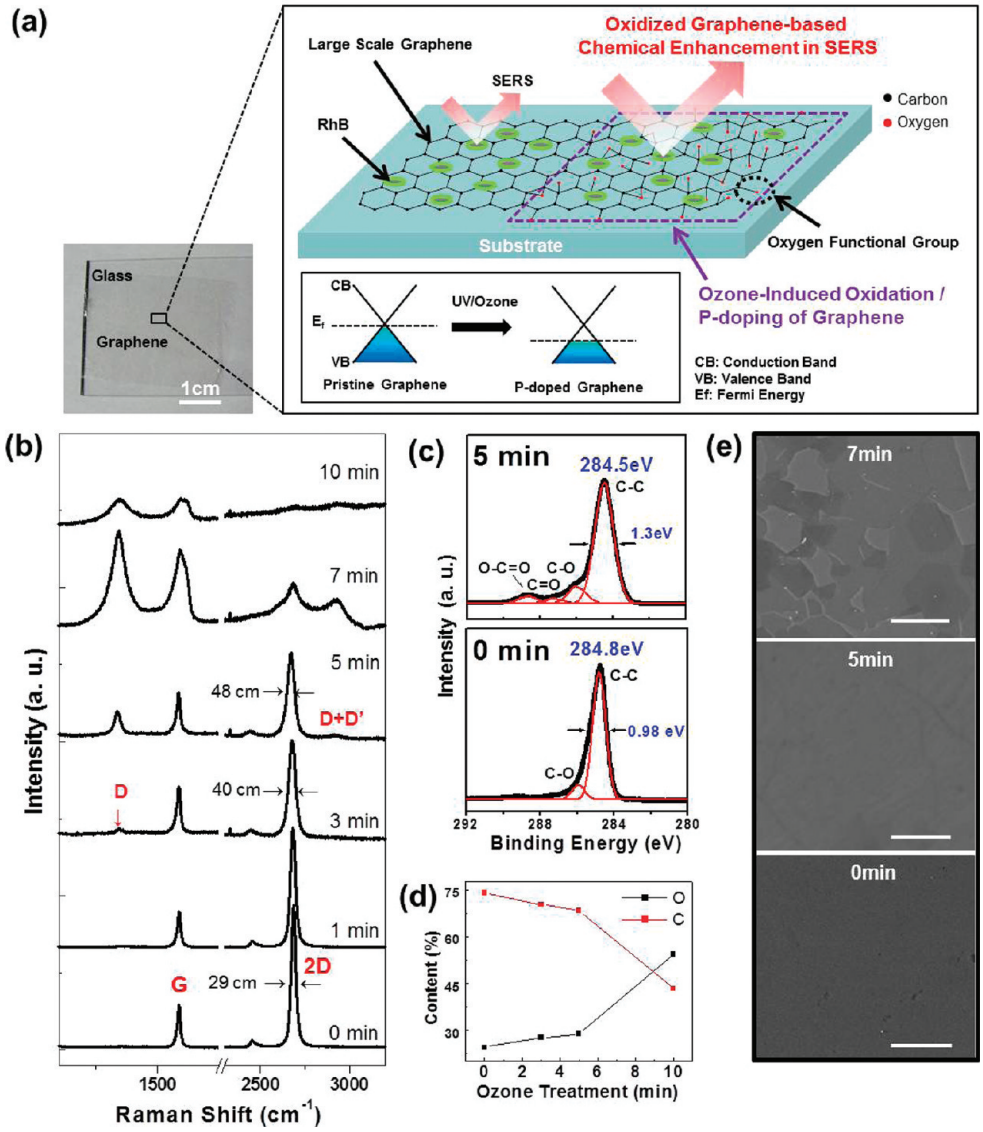

Figure 1. (a) SERS substrate using CVD-grown large-scale graphene. The graphene is oxidized and p-doped by the UV-induced ozone molecules (inset shows the down-shifting of the Fermi energy of the graphene after UV/ozone treatment). RhB molecules are placed on the graphene surface after immersing for 30 min in the aqueous solution (10^{-5} M) and washing with water. The chemical enhancement in SERS on the oxidized graphene is higher than that on the pristine graphene. (b) Change in the Raman spectra of the graphene during the UV/ozone-induced oxidation. (c) XPS spectra of the graphene before and after ozone treatment. (d) Content change in oxygen and carbon as the ozone treatment time increases. (e) SEM images of the graphene substrates after 0, 5, and 7 min ozone treatment. Scale bar is 2 μm.

In this work, we report a straightforward oxidation and patterning strategy for the preparation of large-scale SERS graphene substrates with large chemical enhancement in SERS using the CVD graphene growth and UV/ozone treatment methods (Figure 1). It was reported that ozone molecules, generated by UV-induced oxygen activation,[21−23] can be adsorbed onto the graphene basal plane with a binding energy of 0.25 eV and the physisorbed molecules can chemically react with graphene surface to form oxygen-containing groups including epoxides.[24,25] Notably, we observed that the ozone-induced oxidation of the graphene can contribute to larger chemical SERS enhancement than that from the pristine graphene.[26] We suggest that this oxidation method can provide an efficient and uniform surface oxidation of graphene using the ozone molecules in a site-selective fashion. Raman, X-ray photoelectron spectroscopy (XPS) analyses, and scanning electron microscopy (SEM) were used in characterizing structural changes and chemical groups on the graphene surface during the ozone treatment. Rhodamine B (RhB), rhodamine 6G (R6G), and crystal violet (CV) molecules were used as Raman dyes to study the SERS effect of the graphene surface.[27] In our scheme, the chemical enhancement factors (EFs) can be controlled by UV exposure time for ozone treatment from $\sim 10^3$ to $\sim 10^4$, and 10^4 represents the largest chemical enhancement in SERS ever on a graphene substrate.[5,26]

We suggest that the UV/ozone exposure on the graphene surface provides two different contributions for Raman enhancement: p-type doping effect and oxygen groups. We further proved that SERS signals were rather uniform and reproducible over a centimeter-scale of UV/ozone-oxidized CVD-grown graphene substrate. Finally, a straightforward preparation of micropatterned SERS substrates with large chemical enhancement in SERS using UV/ozone treatment of CVD-grown graphene substrate is shown.

RESULTS AND DISCUSSION

Characterization of Oxidized Graphene and Doping Analysis. Figure 1a shows a schematic diagram of the UV/ozone-oxidized graphene-based chemical enhancement in SERS. The large-scale graphene film was prepared by the CVD method and transferred onto a glass or SiO_2/Si substrate (detailed experimental procedures were described in the Supporting Information and Figure S1).[18] A graphene single layer was confirmed by Raman spectroscopy with 514 nm excitation, showing the two characteristic peaks of graphene, G and 2D bands at ~1580 and ~2680 cm^{-1}, respectively (Figure S2). The intensity ratio of 2D to G band [I(2D)/I(G)] of 3.6 further suggests there is a single-layered graphene.[28,29] The modulation of Raman scattering intensities of molecules on the graphene by tuning the graphene Fermi level with electrical field effect has been reported.[30,31] It was shown that the Raman intensities of the probe molecules become weaker when the graphene Fermi level is up-shifted by applying a positive gate voltage, while they become stronger when the graphene Fermi level is down-shifted by applying a negative gate voltage. In this work, we show that the UV/ozone treatment introduces the strong down-shifting of the graphene Fermi level, indicating the p-type doping of the graphene. Therefore, we suggest that the modulation of the transport properties of the graphene *via* the UV/ozone treatment variation causes the tunable Raman enhancement effect. To obtain the SERS signals on the oxidized graphene, the graphene was immersed in 10^{-5} M RhB solution for 30 min and washed with water. To analyze the structural damage or change of graphene during UV/ozone treatment, Raman, XPS, and SEM studies were performed. Figure 1b shows the evolution of the Raman spectra of the graphene surface as a function of UV/ozone exposure time from 0 to 10 min. It is clear that ozone treatment results in the appearance of sharp D and broad D′ peaks, providing evidence for the degree of disorder in graphene structure.[32] After 5 min, a large deformation was observed in the spectra with strong D and D′ bands. Notably, the Raman spectra showed a gradual decrease of the height and a slight broadening of the 2D bands, which were shown as a change in the ratio of 2D band/G band and in the full width at half-maximum (fwhm) of the 2D band, respectively, and these results indicate that the ozone exposure induced the doping of graphene film.[33,34]

To define the type of doping, we carried out the transport measurements by the device fabrication of graphene field effect transistor (FET) (Figure S3), where the Dirac voltage (the gate dependence of the minimum current) shifts depending on electron or hole doping levels (see the Supporting Information for details).[35,36] Figure S3c shows that the Dirac voltage shifts to a positive value after ozone treatment on graphene, which agrees with the previous result for the p-doping effect of ozone adsorption on graphene.[37] More detailed information about the doping of the ozone-treated graphene was obtained with the XPS spectra (Figure 1c). The results show that the main C1s peak, related to the pure sp^2 carbon−carbon bonds, was down-shifted from 284.8 to 284.5 eV and slightly broadened, caused by p-type doping after 5 min ozone treatment.[30,31] The deconvoluted spectra (red lines in Figure 1c) show the appearance of the oxygen-containing groups on the graphene surface with the bands at 287.3 and 288.7 eV for C═O and O−C═O bonds, respectively, as well as the increased band intensity at 285.9 eV for the C−O bond, contributed from the oxygenated carbon atoms, including epoxide groups, after ozone exposure. The content of oxygen and carbon on the graphene surface was monitored while varying ozone exposure time (Figure 1d). A gradual increase of oxygen and a gradual decrease of carbon up to 5 min ozone exposure were observed, and significant change in content for both oxygen and carbon after 5 min ozone exposure was observed. SEM images further support that the graphene surface had dramatic change in morphology and damage after ozone exposure for >5 min (Figure 1e). These suggest that highly flat graphene surface was mostly preserved up to 5 min ozone treatment with high oxidation on the surface.

Chemical Enhancement-Based SERS Studies on Oxidized Graphene Substrates. Figure 2a shows an actual image of centimeter-scale UV/ozone-exposed graphene substrate (Figure 2a inset), distributions of the 2D band/G band intensity ratios over a large area of the oxidized graphene substrate, and change in SERS intensity at 1648 cm^{-1} (Raman fingerprint peak of RhB molecules) while increasing UV/ozone exposure time from 0 to 7 min. RhB-modified graphene substrate was obtained by immersing the substrate in 10^{-5} M RhB aqueous solution for 30 min and subsequent washing with water, and SERS spectra were obtained with a micro-Raman setup (inVia Raman Microscope, Renishaw, Wotton-under-Edge, UK). First, uniformity and reproducibility in SERS signal at 20 different spots over a 2 cm × 2 cm area of the oxidized graphene substrate were shown as a function of the ozone exposure time at 0, 3, 5, and 7 min (Figure 2a). At 5 min ozone

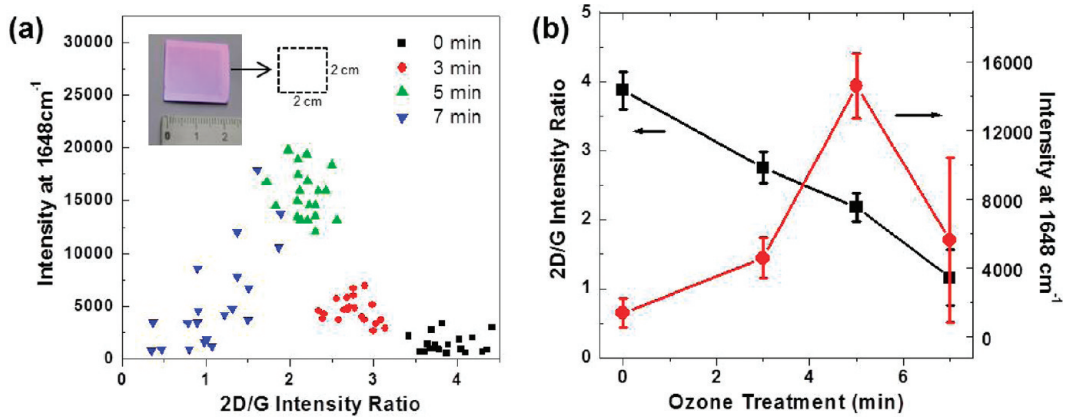

Figure 2. (a,b) Distributions of the SERS intensity at 1648 cm^{-1} from the RhB molecules and 2D band/G band intensity ratio of graphene as a function of the UV/ozone exposure time. The spectra of 20 were obtained on the centimeter-scale graphene substrate in the ozone exposure time of 0, 3, 5, and 7 min (inset of panel a).

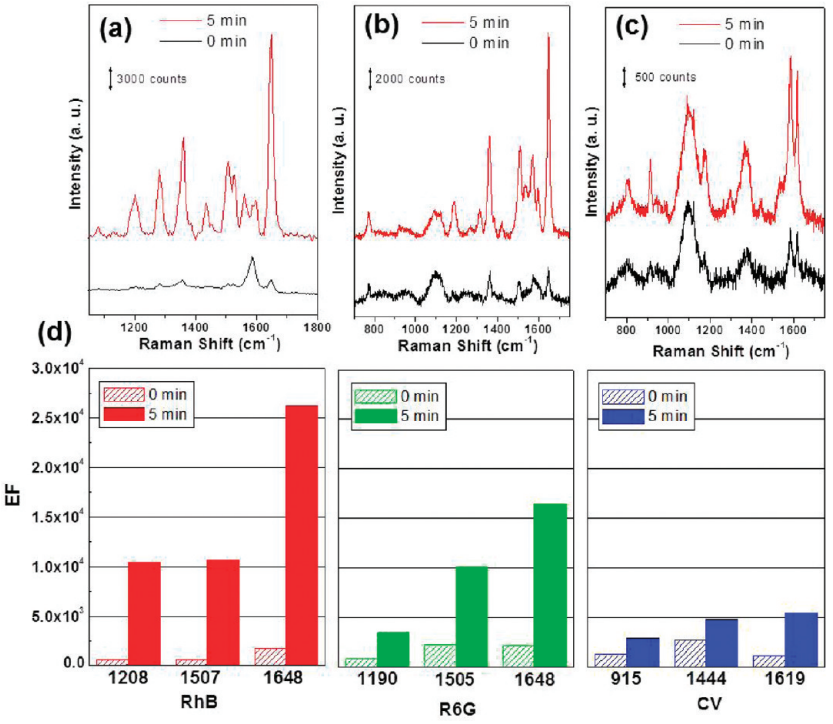

Figure 3. Raman spectra of RhB (a), R6G (b), and CV (c) on the graphene before and after ozone treatment. The graphene was immersed in the 10^{-5} M dye solution before measurement. (d) SERS enhancement factors for RhB, R6G, and CV molecules before and after 5 min ozone treatment.

exposure, the highest SERS signal intensity was observed, but the signal gets weaker when >5 min ozone exposure time was applied to the substrate. Importantly, a distribution of the 2D/G intensity ratio values for 5 min ozone exposure time is relatively narrow over a centimeter area. The highest SERS signal was obtained in ~2.1 ratio, and it was rapidly decreased after 7 min treatment. The ratios in the 0–5 min ozone treatment have a narrow distribution, indicating the uniform ozone treatment on the graphene substrate with signal reproducibility over the whole substrate. The results show that 5 min ozone exposure time is best for obtaining the largest SERS signals with high signal reproducibility over a large area of the oxidized graphene substrate (Figure 2a,b). The 2D/G intensity ratio value was continuously decreased while increasing ozone treatment time.

Next, we studied change in enhancement factors from the Raman dyes on the ozone-oxidized graphene. Figure 3a–c shows the SERS spectra of RhB, R6G, and CV molecules on graphene before and after ozone treatment for 5 min. We found that the Raman intensity of the fingerprint bands of the three Raman dyes was enhanced after 5 min treatment. The RhB molecules

exhibit the vibrational bands corresponding to the aromatic C−C stretching modes at 1648, 1560, 1507, 1433, and 1357 cm^{-1}, a C═C stretching mode at 1595 cm^{-1} (unclearly observed due to the overlapping with the strong G band of graphene at ~1580 cm^{-1}), a C−O−C stretching mode at 1281 cm^{-1}, and an aromatic C−H bending mode at 1208 cm^{-1}.[38,39] Our results suggest that the most increased Raman signals obtained in this spectrum can be assigned to the vibrations related to the benzene rings in RhB molecules, leading to the $\pi-\pi$ interactions with graphene.[40] The R6G molecules exhibit the vibrational bands corresponding to the aromatic C−C stretching modes at 1648, 1572, 1547, 1505, and 1367 cm^{-1}, a C−O−C stretching mode at 1190 cm^{-1}, and an aromatic C−H bending mode at 775 cm^{-1}.[41] The CV molecules exhibit the vibrational bands corresponding to the aromatic C−C stretching modes at 1619, 1585, 1535, and 1444 cm^{-1}, a *N*-phenyl stretching mode at 1370 cm^{-1}, and aromatic C−H bending modes at 1171, 915, and 809 cm^{-1}.[42] Importantly, the SERS EF values in the spectra for all three Raman dyes after ozone treatment showed significant enhancement (Figure 3d; see the Supporting Information for the calculation details of EF values).[43] The EF values for the vibration modes at 1648 cm^{-1} of the RhB and R6G molecules were increased from ~10^3 (1737 and 2161 for RhB and R6G) before ozone treatment to ~10^4 (26265 and 16454 for RhB and R6G) after ozone treatment, and the EF value for the vibration mode at 1619 cm^{-1} of the CV molecules increased from 1126 to 5413 after ozone treatment. Difference in the distance between dye molecule and graphene surface and difference in position and orientation of the highest occupied molecular orbitals and the lowest unoccupied molecular orbitals induce the difference in efficiency of the charge transfer for different dye molecules in the CM of the SERS.[44,45]

To calculate the amount of the adsorbed RhB molecules on the graphene surface before and after ozone treatment, the content of the nitrogen on the RhB-adsorbed graphene surface was monitored by the XPS spectra (Figure S7). We could not observe the noticeable increase in N1s peak in the spectrum before RhB adsorption, and this suggests that the amount of physisorbed N on the oxidized graphene is negligible (Figure S8). The content of nitrogen was consistent from 0 to 5 min ozone exposure but was decreased after 5 min ozone treatment. The results show that CVD-grown graphene surface can be structurally and chemically damaged after >5 min UV/ozone treatment, and the amount of the adsorbed RhB was decreased after a certain amount of ozone exposure time (5 min in this case).

For the large chemical enhancement in SERS for the UV/ozone-treated graphene substrate, we suggest that two different factors contributed to this enhancement: the oxygen groups on graphene surface and the p-type doping of the graphene. Other reports showed that the oxidized graphene provides higher Raman enhancement than the pristine graphene.[26] It was suggested that the oxygen-containing functional groups on the graphene have larger polarizability, and strong local dipole moment for the enhanced local electric field enhances the Raman signal.[46,47] It was also reported that Raman scattering intensity of the probe molecules on the graphene can be controlled by tuning the graphene Fermi level.[48] Down-shifting of the graphene Fermi level was shown therein, indicating the p-type doping, and this leads to larger Raman signal enhancement. The results suggest that the graphene transport system can affect on the Raman scattering signals of the Raman dyes on the graphene. In our work, we showed that both high oxidation and p-doping on CVD-grown graphene were observed after UV/ozone treatment, and both enhancement mechanisms played roles in generating EF values of ~10^4.

Preparation and Characterization of Oxidized Graphene Micropattern. We prepared UV/ozone-induced SERS patterns using the CVD-grown graphene. Figure 4a shows the patterning process of the SERS substrate by ozone treatment. In a typical experiment, first, the graphene film was synthesized by the CVD method (Figure S1) and was transferred onto a SiO_2/Si substrate. Next, poly(methyl methacrylate) (PMMA) was spin-coated on the graphene, and micopatterns were formed by the E-beam lithography through the short lift-off step. The patterned area of the graphene was exposed for UV irradiation, and UV-induced ozone molecules were then interacted with graphene for 0−5 min. After removing the patterned PMMA by acetone, the graphene was immersed in RhB aqueous solution (10^{-5} M) for 30 min. After washing with deionized water, the patterned SERS substrate was formed. Figure 4b shows the side view of the schematic representation for the RhB-adsorbed graphene SERS substrate with a micropattern. The optical microscope image of the graphene with patterned PMMA is shown in Figure 4c before the patterned PMMA was removed. The UV-irradiated area (for 5 min; area A) and PMMA-masked area (area B) are shown in Figure 3c.

To observe the selective ozone patterning and subsequent Raman enhancement in the ozone-treated area, Raman spectra were mapped and integrated with the characteristic peaks of RhB molecule (1648, 1360, and 1280 cm^{-1}) (Alpha 300s, WITEC, Ulm, Germany; Figure 4d−f). The Raman mapping images with three different characteristic peaks matched well and clearly showed the micropatterns with ozone-treated and masked areas.

In summary, we found that simple UV/ozone treatment can selectively induce highly efficient oxidation in preparing a large SERS-active graphene substrate, and this oxidation along p-doping can result in

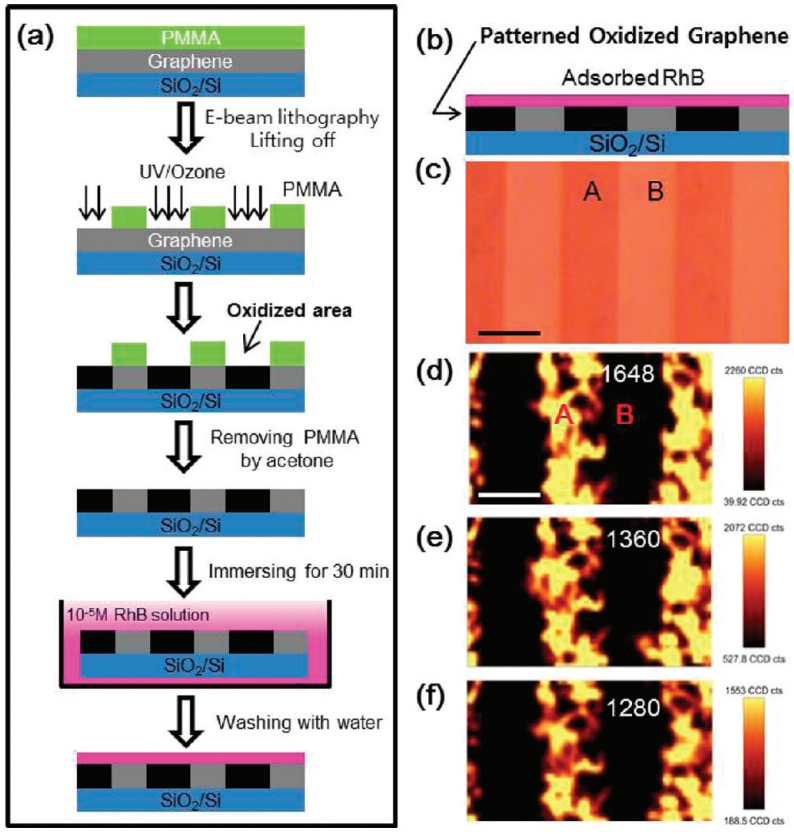

Figure 4. (a) UV/ozone-induced oxidation and patterning process of the graphene substrate. PMMA film on the CVD-grown graphene surface was micropatterned by E-beam lithography and lifting off. It provides selective oxidation of the graphene during UV/ozone exposure. After removing PMMA by acetone, this patterned substrate is immersed in 10^{-5} M RhB solution for 30 min. After washing with deionized water, RhB molecules were adsorbed on the patterned-oxidized graphene substrate (b). (c) Optical microscope image of the graphene with the patterned PMMA by E-beam lithography. Area A is the UV-exposed area, and area B is the PMMA-covered area. Raman images were mapped with the integrated intensities of the characteristic peaks of RhB molecules on the graphene substrate with 5 min ozone treatment [(d) 1468, (e) 1360, and (f) 1280 cm^{-1}]. Scale bar is 5 μm.

very high SERS signal. To the best of our knowledge, this is the first example of using UV/ozone-oxidized large-scale graphene patterns for chemical SERS enhancement study. Moreover, the chemical enhancement factor reported herein is $\sim 10^4$, the largest ever on graphene—at least 1 order of magnitude higher than any other examples. Moreover, this strategy can be readily applicable to a CVD-grown large-scale graphene surface with a straightforward patterning capability, and strong SERS signals were detected over a large area in a rather reproducible fashion. The SERS enhancement was gradually increased as ozone exposure time was increased, showing a straightforward control of oxidation on graphene and tunability of chemical enhancement on the SERS-active graphene platform using our strategy. Finally, a UV/ozone treatment on CVD-grown graphene can readily and efficiently generate a large-scale SERS substrate with high SERS signals within ozone-treated areas while keeping very low SERS signals in nontreated areas. This large-scale graphene platform with large chemical enhancement in SERS can be readily coupled to plasmonic nanostructures with large electromagnetic enhancement in SERS[49−51] for the ultrasensitive and quantitative SERS sensing applications.

EXPERIMENTAL SECTION

Synthesis of Graphene. The graphene films were synthesized on Cu foils by the CVD method as previously reported.[18] The Cu foils (25 μm thickness) were placed in a quartz tube under an argon atmosphere. The temperature was increased to 1000 °C, and the reaction gas mixture of CH_4 and H_2 was flowed. Then, the foils were cooled to room temperature with a rate of ~10 °C. Since the graphene layers are formed on both sides of a Cu foil, the back side graphene should be removed by O_2 plasma etching after protecting the front graphene layer with PMMA. After the Cu foil was etched in an ammonium persulfate solution for ~10 h, the graphene layer was transferred onto a target substrate. Finally, the PMMA layer was removed by acetone.

Preparation of the Patterned SERS Substrates. To pattern the PMMA film on the graphene, E-beam lithography was used (JSM-7401F; JEOL). A microsized stripe-patterned PMMA was attached onto the graphene surface as a shadow mask before irradiation with UV light source (UV/ozone cleaner, Bioforce). After PMMA pattern was removed from the film surface by acetone, the graphene film was immersed in 10^{-5} M RhB

(Sigma-Aldrich, 95%) aqueous solution for 30 min and washed with deionized water to remove nonbonded RhB molecules on the graphene surface. Raman images for the integrated intensities of the fingerprints of the RhB molecule on the patterned SERS substrate were mapped by using Alpha 300s (WITEC, Ulm, Germany) with Ar laser of 514 nm at the power of 1.5 mW and pixel size of 250 nm. Other Raman dyes (R6G and CV) were also purchased from Sigma-Aldrich for additional SERS experiments.

Measurements. The Raman spectra were acquired using Renishaw inVia Raman Microscope with Ar laser of 514 nm at the power of 1.6−16 mW and laser spot size of 2 μm. The morphologies of the graphene films during the ozone treatment were determined by using scanning electron microscope (SEM) operating at an accelerating voltage of 5 kV. The X-ray photoelecton spectroscopy (XPS) was used for measurement of binding energy of the carbon bond (ThermoVG, UK). The gate-dependent current of the films was measured with probe station at room temperature.

Acknowledgment. This work was supported by 21C Frontier Functional Proteomics Project (FPR08-A2-150) through the National Research Foundation of Korea (NRF) from the Ministry of Education, Science and Technology (2011K00135), the National Research Foundation of Korea (NRF) grant funded by the Korea government (MEST) (2011-0018198), and the Industrial Core Technology Development Program of the Ministry of Knowledge Economy (Nos. 10033183 and 10037397). This work was additionally supported by the KRICT OASIS Project from the Korea Research Institute of Chemical Technology. K. S. Kim was supported by NRF (National Honor Scientist Program: 2010-0020414), and B. H. Hong was supported by the National Research Foundation of Korea (NRF) grant funded by the Korea government (MEST) (2011K000615).

Supporting Information Available: CVD-based graphene growth, electrical measurement on graphene FET, Raman spectra of dye molecules, SERS spectra of RhB molecules on graphene, calculation method for SERS enhancement factors, XPS spectra of graphene, RhB molecule distribution images on graphene, and a table for change in SERS intensity and EFs of RhB molecules on graphene while varying ozone exposure time. This material is available free of charge *via* the Internet at http://pubs.acs.org.

REFERENCES AND NOTES

1. Novoselov, K. S.; Geim, A. K.; Morozov, S. V.; Jiang, D.; Zhang, Y.; Dubonos, S. V.; Grigorieva, I. V.; Firsov, A. A. Electric Field Effect in Atomically Thin Carbon Films. *Science* **2004**, *306*, 666–669.
2. Geim, A. K.; Novoselov, K. S. The Rise of Graphene. *Nat. Mater.* **2007**, *6*, 183–191.
3. Novoselov, K. S.; Geim, A. K.; Morozov, S. V.; Jiang, D.; Katsnelson, M. I.; Grigorieva, I. V.; Dubonos, S. V.; Firsov, A. A. Two-Dimensional Gas of Massless Dirac Fermions in Graphene. *Nature* **2005**, *438*, 197–200.
4. Zhang, Y.; Tan, Y. W.; Stormer, H. L.; Kim, P. Experimental Observation of the Quantum Hall Effect and Berry's Phase in Graphene. *Nature* **2005**, *438*, 201–204.
5. Ling, X.; Xie, L. M.; Fang, Y.; Xu, H.; Zhang, H. L.; Kong, J.; Dresselhaus, M. S.; Zhang, J.; Liu, Z. F. Can Graphene Be Used as a Substrate for Raman Enhancement?. *Nano Lett.* **2010**, *10*, 553–561.
6. Xie, L. M.; Ling, X.; Fang, Y.; Zhang, J.; Liu, Z. F. Graphene as a Substrate To Suppress Fluorescence in Resonance Raman Spectroscopy. *J. Am. Chem. Soc.* **2009**, *131*, 9890–9891.
7. Ling, X.; Zhang, J. First-Layer Effect in Graphene-Enhanced Raman Scattering. *Small* **2010**, *6*, 2020–2025.
8. Zhou, H.; Qiu, C.; Yu, F.; Yang, H.; Chen, M.; Hu, L.; Sun, L. Thickness-Dependent Morphologies and Surface-Enhanced Raman Scattering of Ag Deposited on n-Layer Graphenes. *J. Phys. Chem. C* **2011**, *115*, 11348–11354.
9. Nie, S.; Emory, S. R. Probing Single Molecules and Single Nanoparticles by Surface-Enhanced Raman Scattering. *Science* **1997**, *275*, 1102–1106.
10. Kneipp, K.; Wang, Y.; Kneipp, H.; Perelman, L. T.; Itzkan, I.; Dasari, R. R.; Feld, M. S. Single Molecule Detection Using Surface-Enhanced Raman Scattering (SERS). *Phys. Rev. Lett.* **1997**, *78*, 1667–1670.
11. Campion, A.; Kambhampati, P. Surface-Enhanced Raman Scattering. *Chem. Soc. Rev.* **1998**, *27*, 241–251.
12. Moskovits, M. Surface-Enhanced Raman Spectroscopy: A Brief Retrospective. *J. Raman Spectrosc.* **2005**, *36*, 485–496.
13. Otto, A.; Mrozek, I.; Grabhorn, H.; Akemann, W. Surface-Enhanced Raman Scattering. *J. Phys: Condens. Matter* **1992**, *4*, 1143–1212.
14. Sun, Y. H.; Liu, K.; Miao, J.; Wang, Z. Y.; Tian, B. Z.; Zhang, L. N.; Li, Q. Q.; Fan, S. S.; Jiang, K. L. Highly Sensitive Surface-Enhanced Raman Scattering Substrate Made from Superaligned Carbon Nanotubes. *Nano Lett.* **2010**, *10*, 1747–1753.
15. Saikin, S. K.; Chu, Y.; Rappoport, D.; Crozier, K. B.; Aspuru-Guzik, A. Separation of Electromagnetic Chemical Contributions to Surface-Enhanced Raman Spectra on Nanoengineered Plasmonic Substrates. *J. Phys. Chem. Lett.* **2010**, *1*, 2740–2746.
16. Bruna, M.; Borini, S. Optical Constants of Graphene Layers in the Visible Range. *Appl. Phys. Lett.* **2009**, *94*, 031901.
17. Rana, F. Graphene Terahertz Plasmon Oscillators. *IEEE Trans. Nanotechnol.* **2008**, *7*, 91–99.
18. Kim, K. S.; Zhao, Y.; Jang, H.; Lee, S. Y.; Kim, J. M.; Kim, K. S.; Ahn, J. H.; Kim, P.; Choi., J. Y.; Hong, B. H. Large-Scale Pattern Growth of Graphene Films for Stretchable Transparent Electrodes. *Nature* **2009**, *457*, 706–710.
19. Li, X.; Zhu, Y.; Cai, W.; Borysiak, M.; Han, B.; Chen, D.; Piner, R. D.; Colombo, L.; Ruoff, R. S. Transfer of Large-Area Graphene Films for High-Performance Transparent Conductive Electrodes. *Nano Lett.* **2009**, *9*, 4359–4363.
20. Lee, W. H.; Park, J.; Sim, S. H.; Jo, S. B.; Kim, K. S.; Hong, B. H.; Cho, K. Transparent Flexible Organic Transistors Based on Monolayer Graphene Electrodes on Plastic. *Adv. Mater.* **2011**, *23*, 1752–1756.
21. Mawhinney, D. B.; Naumenko, V.; Kuznetsova, A.; Yates, J. T.; Liu, J.; Smalley, R. E. Infrared Spectral Evidence for the Etching of Carbon Nanotubes: Ozone Oxidation at 298 K. *J. Am. Chem. Soc.* **2000**, *122*, 2383–2383.
22. Simmons, J. M.; Nichols, B. M.; Baker, S. E.; Marcus, M. S.; Castellini, O. M.; Lee, C. S.; Hamers, R. J.; Eriksson, M. A. Effect of Ozone Oxidation on Single-Walled Carbon Nanotubes. *J. Phys. Chem. B* **2006**, *110*, 7113–7118.
23. Wongwiriyapan, W.; Honda, S.; Konishi, H.; Mizuta, T.; Ikuno, T.; Ohmori, T.; Ito, T.; Shimazaki, R.; Maekawa, T.; Suzuki, K.; *et al.* Ultrasensitive Ozone Detection Using Single-Walled Carbon Nanotube Networks. *Jpn. J. Appl. Phys.* **2006**, *45*, 3669–3671.
24. Leconte, N.; Moser, J.; Ordejon, P.; Tao, H.; Lherbier, A.; Bachtold, A.; Alsina, F.; Torres, C. M. S.; Charlier, J. C.; Roche, S. Damaging Graphene with Ozone Treatment: A Chemically Tunable Metal-Insulator Transition. *ACS Nano* **2010**, *4*, 4033–4038.
25. Lee, G.; Lee, B.; Kim, J.; Cho, K. Ozone Adsorption on Graphene: *Ab Initio* Study and Experimental Validation. *J. Phys. Chem. C* **2009**, *113*, 14225–14229.
26. Yu, X.; Cai, H.; Zhang, W.; Li, X.; Luo, Y.; Wang, X.; Hou, J. G. Tuning Chemical Enhancement of SERS by Controlling the Chemical Reduction of Graphene Oxide Nanosheets. *ACS Nano* **2011**, *5*, 952–958.
27. Lee, P. C.; Meisel, D. Adsorption and Surface-Enhanced Raman of Dyes on Silver and Gold Sols. *J. Phys. Chem.* **1982**, *86*, 3391–3395.
28. Pisana, S.; Lazzeri, M.; Casiraghi, C.; Novoselov, K. S.; Geim, A. K.; Ferrari, A. C.; Mauri, F. Breakdown of the Adiabatic Born−Oppenheimer Approximation in Graphene. *Nat. Mater.* **2007**, *6*, 198–201.
29. Das, A.; Pisana, S.; Chakraborty, B.; Piscanec, S.; Saha, S. K.; Waghmare, U. V.; Novoselov, K. S.; Krishnamurthy, H. R.; Geim, A. K.; Ferrari, A. C.; *et al.* Monitoring Dopants by Raman Scattering in an Electrochemically Top-Gated Graphene Transistor. *Nat. Nanotechnol.* **2008**, *3*, 210–215.

30. Choudhury, D.; Das, B.; Sarma, D. D.; Rao, C. N. R. XPS Evidence for Molecular Charge-Transfer Doping of Graphene. *Chem. Phys. Lett.* **2010**, *497*, 66–69.
31. Walter, A. L.; Jeon, K. J.; Bostwick, A.; Speck, F.; Ostler, M.; Seyller, T.; Moreschini, L.; Kim, Y. S.; Chang, Y. J.; Horn, K.; *et al.* Highly p-Doped Epitaxial Graphene Obtained by Fluorine Intercalation. *Appl. Phys. Lett.* **2011**, *98*, 184102.
32. Elias, D. C.; Nair, R. R.; Mohiuddin, T. M. G.; Morozov, S. V.; Blake, P.; Halsal, M. P.; Ferrari, A. C.; Boukhvalov, D. W.; Katsnelson, M. I.; Geim, A. K.; *et al.* Control of Graphene's Properties by Reversible Hydrogenation: Evidence for Graphane. *Science* **2009**, *323*, 610–613.
33. Schedin, F.; Lidorikis, E.; Lombardo, A.; Kravets, V. G.; Geim, A. K.; Grigorenko, A. N.; Novoselov, K. S.; Ferrari, A. C. Surface-Enhanced Raman Spectroscopy of Graphene. *ACS Nano* **2010**, *4*, 5617–5626.
34. Ferrari, A. C.; Meyer, J. C.; Scardaci, V.; Casiraghi, C.; Lazzeri, M.; Mauri, F.; Piscanec, F.; Jiang, D.; Novoselov, K. S.; Roth, S.; *et al.* Raman Spectrum of Graphene and Graphene Layers. *Phys. Rev. Lett.* **2006**, *97*, 187401.
35. McCreary, K. M.; Pi1, K.; Swartz, A. G.; Han, W.; Bao, W.; Lau, C. N.; Guinea, F.; Katsnelson, M. I.; Kawakami, R. K. Effect of Cluster Formation on Graphene Mobility. *Phys. Rev. B* **2010**, *81*, 115453.
36. Pi, K.; Han, W.; McCreary, K. M.; Swartz, A. G.; Li, Y.; Kawakami, R. K. Manipulation of Spin Transport in Graphene by Surface Chemical Doping. *Phys. Rev. Lett.* **2010**, *104*, 187201.
37. Yan, J.; Zhang, Y.; Kim, P.; Pinczuk, A. Electric Field Effect Tuning of Electron−Phonon Coupling in Graphene. *Phys. Rev. Lett.* **2007**, *98*, 166802.
38. Hildebrandt, P.; Stockburger, M. Surface-Enhanced Resonance Raman Spectroscopy of Rhodamine 6G Adsorbed on Colloidal Silver. *J. Phys. Chem.* **1984**, *88*, 5934–5944.
39. Ke, Y. K.; Dong, H. R. *Analytic Chemistry-Spectrum Analysis*; Chemical Industry Press: Beijing, 1998; p 1158.
40. Ichii, T.; Hosokawa, Y.; Kobayashi, K.; Matsushige, K.; Yamada, H. Molecular-Resolution Imaging of Lead Phthalocyanine Molecules by Small Amplitude Frequency Modulation Atomic Force Microscopy Using Second Flexural Mode. *Appl. Phys. Lett.* **2009**, *94*, 133110.
41. Majoube, M.; Henrya, M. Fourier Transform Raman and Infrared and Surface-Enhanced Raman Spectra for Rhodamine 6G. *Spectrochim. Acta, Part A* **1991**, *47*, 1459–1466.
42. Angeloni, L.; Smulevich, G.; Marzocchi, M. P. Resonance Raman Spectrum of Crystal Violet. *J. Raman Spectrosc.* **1979**, *8*, 305–310.
43. Fang, Y.; Seong, N.-H.; Dlott, D. D. Measurement of the Distribution of Site Enhancements in Surface-Enhanced Raman Scattering. *Science* **2008**, *321*, 388–392.
44. Otto, A. The `Chemical' (Electronic) Contribution to Surface-Enhanced Raman Scattering. *J. Raman Spectrosc.* **2005**, *36*, 497–507.
45. Mrozek, I.; Otto, A. Long- and Short-Range Effects in SERS from Silver. *Europhys. Lett.* **1990**, *11*, 243–248.
46. Bottcher, C. J. F. *Theory of Electric Polarization*; Elesevier: Amsterdam, 1973; pp 17−26.
47. Nir, S.; Adams, S.; Rein, R. Polarizability Calculations on Water, Hydrogen, Oxygen and Carbon Dioxide. *J. Chem. Phys.* **1973**, *59*, 3341–3355.
48. Xu, H.; Xie, L.; Zhang, H.; Zhang, J. Effect of Graphene Fermi Level on the Raman Scattering Intensity of Molecules on Graphene. *ACS Nano* **2011**, *5*, 5338–5344.
49. Lim, D.-K.; Jeon, K.-S.; Kim, H.-M.; Nam, J.-M.; Suh, Y. D. Nanogap-Engineerable Raman-Active Nanodumbbells for Single-Molecule Detection. *Nat. Mater.* **2010**, *9*, 60.
50. Lim, D.-K.; Jeon, K.-S.; Hwang, J.-H.; Kim, H.; Kwon, S.; Suh, Y. D.; Nam, J.-M. Highly Uniform and Reproducible Surface-Enhanced Raman Scattering from DNA-Tailorable Nanoparticles with 1-nm Interior Gap. *Nat. Nanotechnol.* **2011**, *6*, 452.
51. Tan, S. J.; Campolongo, M. J.; Luo, D.; Cheng, W. Building Plasmonic Nanostructures with DNA. *Nat. Nanotechnol.* **2011**, *6*, 268.